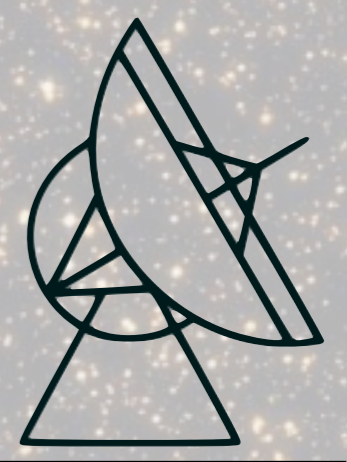




Resolving the circumstellar environment of the B[e] star V921 Sco with VLT/AMBER

A. Kreplin⁽¹⁾, S. Kraus⁽²⁾, K.-H. Hofmann⁽¹⁾, D. Schertl⁽¹⁾, G. Weigelt⁽¹⁾, and T. Driebe⁽³⁾

(1) Max-Planck-Institut für Radioastronomie, Bonn, Germany
 (2) Department of Astronomy, University of Michigan, Ann Arbor, USA
 (3) Deutsches Zentrum für Luft- und Raumfahrt, Bonn, Germany



Max-Planck-Institut für Radioastronomie

MAX-PLANCK-GESELLSCHAFT

Introduction

The southern emission-line star V921 Sco (CD-42°11721, MWC 865, He 3-1300) is an intermediate-mass object with $M_* = 8 - 10 M_\odot$ (Borges Fernandes et al. 2007). The existence of a strong H β line was first reported by Merrill & Burwell (1949), who also noted the peculiar spectrum of this object. Surrounded by a small nebula (Glass & Allen 1975), V921 Sco resembles objects belonging to the class of intermediate-mass young stellar objects, the Herbig Ae/Be stars (Herbig 1960). While Finkenzeller & Mundt (1984) classified V921 Sco as a Herbig Be star, Hutsemekers & van Drom (1990) pointed out its similarity to Be supergiants. The main uncertainties concerning the true nature of V921 Sco are the not well-known stellar parameters and the rough distance estimate.

New OPD correction method

V921 Sco was observed with the VLT/AMBER instrument (Petrov et al. 2007) on three nights in May 2007. The observations were carried out using three of the auxiliary 1.8 m telescopes (ATs) of the VLT, arranged in linear configuration ($B_1 = 31.2$ m, $B_2 = 62.6$ m, $B_3 = 93.8$ m). The AMBER data were taken in the low-spectral resolution mode ($R = 35$), allowing us to observe in the H and K bands simultaneously.

Since the coherence length of AMBER LR observations is only approximately 60 to 80 μ m, while the atmospheric piston in our data is of the order of 20 μ m, we cannot neglect the influence of the optical path differences (OPDs) between the beams on the visibility calibration. To take care of this effect, we developed a method which is able to partially correct systematic differences between OPD errors of the target and calibrator data.

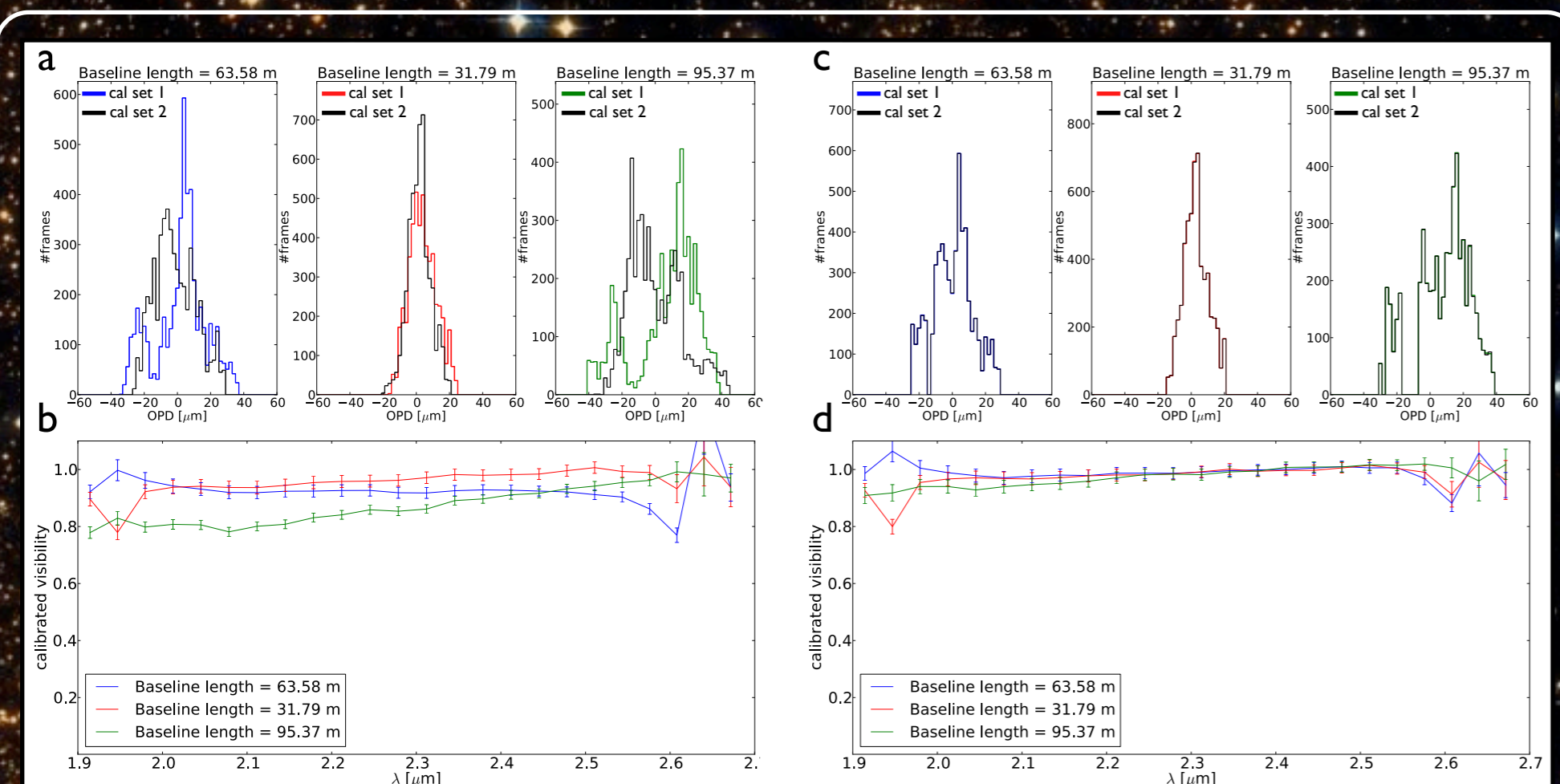


Figure 1: Test of the OPD histogram equalization with two different data sets of the calibrator HD 127753. **a:** OPD histograms of the two data sets. **b:** Computed visibilities obtained without OPD histogram equalization. **c:** OPD histogram obtained after the histogram equalization was applied to the data sets. **d:** Computed visibilities obtained after the OPD histogram equalization was applied.

If the raw frames of the science target and the calibrator would have nearly the same histogram of OPD values, the visibility transfer function of both would be nearly identical, and therefore would not much degrade the visibility calibration. Therefore, we improve our visibility calibration by performing an equalization of the OPD histograms (see Fig. 1) of target and calibrator (see Kreplin et al. 2011 for more details).

The circumstellar environment of V921 Sco

To characterize the size of V921 Sco's circumstellar environment, we fit a ring model to the observed visibilities. In the size-luminosity relation (Fig. 3), the fitted ring radius (inner radius of a ring with a width of 20% of the inner radius) of V921 Sco is plotted using the stellar parameters given by Borges Fernandes et al. (2007). If we assume that these stellar parameters are correct, the position of V921 Sco in the size-luminosity diagram suggests that the K band ring-fit radius (2.10 mas / 2.41 AU) is nearly equal or only slightly smaller (~ 1.5 times) than the theoretical dust sublimation radius expected in the absence of radiation-shielding material between the star and the disk.

In addition to the geometrical modeling described above, a temperature-gradient model of a disk with an inner cavity is also able to reproduce the wavelength-dependent visibilities and the SED of V921 Sco (see parameters in Fig. 2).

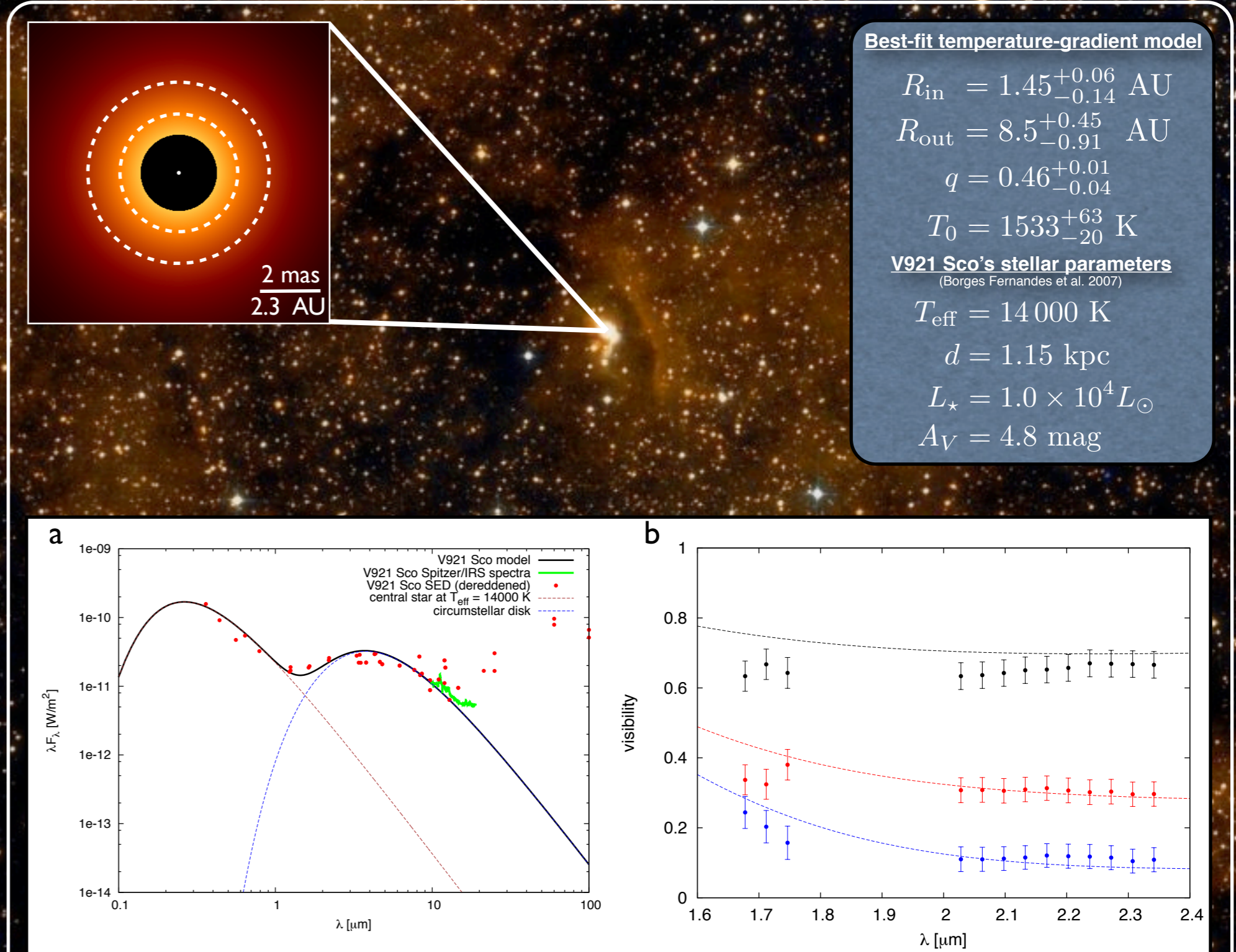


Figure 2: AMBER visibilities, SED, and best-fit temperature-gradient model of V921 Sco. **a:** wavelength-dependent calibrated visibilities (baselines 31 m, 63 m, 95 m from top to bottom) and temperature-gradient model fits. **b:** available ground-based SED data, Spitzer spectrum (green line), and the model fit (black line). The inset shows the K-band intensity distribution of the best-fit temperature-gradient model (log scaling). The white dashed rings indicate the dust sublimation radii predicted by the size-luminosity relation for the temperatures of 1500 K (outer ring) and 2000 K (inner ring) using the stellar parameters reported by Borges Fernandes et al. (2007).

If the inner radius of V921 Sco is really more compact than the sublimation radius, as suggested for several other B[e] stars, this compact observed size can be explained by either (1) a bright additional disk component inside the dust sublimation region contributing to the total emission, or (2) an inner disk component that partially shields the radiation from the central star leading to a smaller dust sublimation radius (Akeson et al. 2005; Monnier et al. 2005; Kraus et al. 2008b; Benisty et al. 2010; Weigelt et al. 2011).

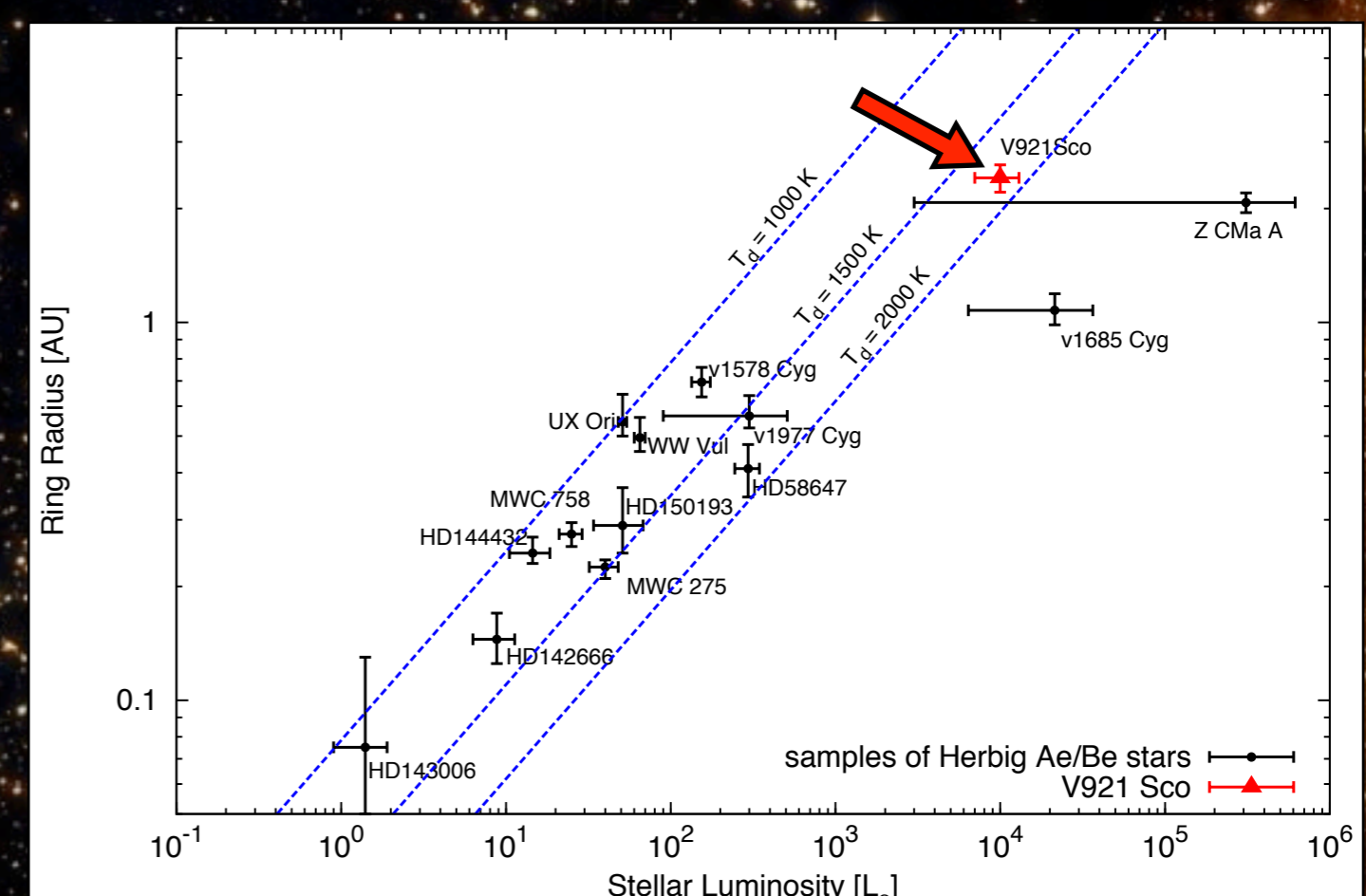


Figure 3: Size-luminosity diagram of a sample of Herbig Ae/Be stars (adopted from Monnier et al. 2005). The K-band ring-fit radius of V921 Sco determined in this paper is plotted as a red triangle (see arrow). The dotted blue lines represent model curves for three different dust sublimation temperatures. We note that the distance and luminosity of V921 Sco are very uncertain. The plotted red error bar represents the parameter uncertainty reported in Borges Fernandes et al. (2007), but the total uncertainty is probably larger.

References

- Akeson, R. L., et al. 2005, *ApJ* 622, 440A
 Benisty, M., et al. 2010, *A&A* 511A, 74B
 Borges Fernandes, M., et al. 2007, *MNRAS* 377, 1343
 Finkenzeller, U. & Mundt, R. 1984, *A&AS* 55, 109
 Glass, I. S. & Allen, D. A., 1975, *Obs.* 95, 27G
 Hutsemekers, D. & van Drom, E. 1990, *A&A* 238, 134
 Kraus, S., et al. 2008, *A&A* 489, 1157
 Kreplin, A., et al. 2011, *A&A* in press
 Merrill, P. W. & Burwell, C. G. 1949, *ApJ* 110, 387
 Millan-Gabet, R., et al. 2007, *PPV* 539
 Monnier, J., et al. 2005, *ApJ* 624, 832
 Petrov, R., et al. 2007, *A&A* 464, 1P
 Weigelt, G., et al. 2011, *A&A* 527A, 103W